Measurement of muonic and electromagnetic components in cosmic ray air showers using LHAASO-KM2A prototype array

Cong Li,[1,2,*] Huihai He,[1,2,†] Gang Xiao,[2] Shaohui Feng,[2] Xiong Zuo,[2] Lingyu Wang,[2] Yi Zhang,[2] Xiurong Li,[2] Ning Cheng,[2] Song-Zhan Chen,[2] Zhe Li,[2] Jia Liu,[2] Hongkui Lv,[2] Xiangdong Sheng,[2] Sha Wu,[1,2] Wei Gao,[1,2] Yuncheng Nan,[1,2] Jinfan Chang,[2] Wei Wang,[2] Minghao Gu,[2] Fei Li,[2] Mohsin Saeed,[2] Hongming Li,[3] Guanghua Gong,[3] Shaoru Zhang,[4] and Hui Wang[5]

(LHAASO Collaboration)

[1]*University of Chinese Academy of Sciences, Beijing, 100049, China*
[2]*Key Laboratory of Particle Astrophyics, Institute of High Energy Physics, Chinese Academy of Sciences, Beijing, 100049, China*
[3]*Tsinghua University, Beijing, 100084, China*
[4]*Hebei Normal University, Shijiazhuang, 050024, China*
[5]*Southwest Jiaotong University, Chengdu, 611756, China*

(Received 9 April 2018; published 6 August 2018)

A LHAASO-KM2A prototype array, which is about 1% of the full one, had been in stable operation for about 3 years from 2014 to 2016. This work presents a combined measurement of shower muons and electromagnetic particles using its data. Benefiting from the wide dynamic range of the muon detectors and the surrounding electromagnetic detector array, the muon content was studied in detail for showers with energies from tens of TeV to tens of PeV. The results are compatible with the prediction of Monte Carlo simulation and no obvious excess is observed when taking into account that the mass composition increases above 1 PeV. The results also support a transition from light to heavy elements for cosmic rays in the "knee" region.

DOI: 10.1103/PhysRevD.98.042001

I. INTRODUCTION

Due to the rapidly decreasing flux with increasing energy, the study of high-energy cosmic rays at energies above 10^{14} eV is difficult for space-born experiments and mainly relies on measurements of the induced extensive air shower (EAS) on ground [1]. To reconstruct the properties of primary cosmic rays, simulations of the shower development should be used, which are strongly related to the hadronic interaction models [2]. Unfortunately, most of the observables in EAS experiments involve processes with small transverse momenta where QCD cannot be applied perturbatively [3]. Instead, phenomenological models based on accelerator data are invoked. As a result, these models are limited by experimental data, especially at higher energy and in the very forward region where accelerator data cannot completely cover [4,5]. In the previous measurements of EAS parameters especially for mass composition study, the inconsistency between different hadronic interaction models has been the main sources of uncertainties [2,6].

Actually, EAS experiments can also be used to test hadronic interaction models. Muons are the decay products of hadrons and undergo less atmosphere interactions than electromagnetic particles, which makes them ideal "probes" to understand the hadronic interaction processes [3]. Many tests were performed using muon data and discrepancies between experiment measurements and models were found by different experiments, in which the muon bundle excess compared to simulation is a long-standing problem for air shower experiments [7]. At ultrahigh energy, a clear excess of muon production comparing to simulation was reported by Auger experiment [8] and HiRes/MIA experiment [9]. Yakutsk experiment also indicated that the simulated muon densities is lower than observed [10]. As for detectors working at lower energies, such as the KSCADE-GRANDE experiment, different hadronic interaction models were tested systematically [11] and there were clear differences between different models [2]. None of the models could consistently describe the observed rates of electron and muon numbers over the whole energy range [12] and the dependence of the muon content with zenith angle showed clear conflicts in inclined showers [3]. However, the results from IceTop [13] and EAS-MSU [14] showed there no evidence for a significance muon excess. Some other important results were from underground particle physics detectors at colliders. The ALEPH and DELPHI groups

*licong@ihep.ac.cn
†hhh@ihep.ac.cn

found that the production rate for the highest multiplicity events is higher than expectation even assuming a purely iron primary composition [15,16].

Several suggestions were proposed to explain these discrepancies. Some theorists suggested the presence of nuggets of strange quark matter in very high energy cosmic rays [17], while others tried to involve creation of the QGP in interactions and so on [18–20]. The hadronic interaction models have indeed made many changes especially after the release of LHC data, and the main change related to muon content in models is the enhancement of production of ρ^0 vector mesons which may lead to suppression of production of π^0 mesons [21,22]. Contrary to the scalar π^0, the dominant decay channel for ρ^0 is $\rho^0 \to \pi^-\pi^+$, so the enhancement of ρ^0 production can enrich the production of muons, but a suppression of the electromagnetic component is a cumulative effect. Therefore, it is better to test the muon and electromagnetic components simultaneously. It should be noted that the ALICE experiment has repeated the work performed by ALEPH and DELPHI groups, and there is no clear excess of high muon multiplicity events compared to simulation [23], which may benefit from the progress in hadronic interaction models, but their results were limited by large uncertainties. On the other hand, there is still clear excess observed in ultrahigh energy [24–26] even compared with the newest models, and the muon content attenuation in atmosphere is still lower than predicted for KASCADE-Grande experiment [27].

LHAASO (Large High Altitude Air Shower Observatory) is a ground-based air shower observatory which aims to study the high energy cosmic rays from 10^{13} eV to 10^{17} eV, and this new experiment can also continuously survey the gamma-ray sky from about 100 GeV to 1 PeV [28]. For this, LHAASO will need to separate hadronic showers from electromagnetic showers [29] at energies up to PeV, thus a reliable hadronic interaction model is very important for LHAASO both from the aspects of cosmic ray study and VHE gamma-ray astronomy. LHAASO is a hybrid array which consists of an EAS array covering an area about 1.3 km^2 (KM2A), 78000 m^2 water Cherenkov detector array (WCDA) and 12 wide-filed air Cherenkov/fluorescence telescopes (WFCTA) [30].

LHAASO-KM2A is comprised of 5195 scintillation detectors (EDs) and 1171 muon detectors (MDs). One of the scientific motivations of KM2A is to study cosmic rays with energies from 10 TeV to 100 PeV, so the dynamic range for a detector unit needs to span 4 orders of magnitude [31]. To study the performances of detector and prepare for LHAASO-KM2A construction, a prototype array was constructed at YBJ cosmic ray observatory in 2014. The newest model is tested using the prototype array data. In this work, we take advantage of the large dynamic range of the muon detector and the electromagnetic particle detector array to study muonic and electromagnetic components of EAS in a wide energy range. The electromagnetic detectors are also used to provide rough information about the core, direction and energy of shower, which are crucial to minimize punch-through effect from high energy electromagnetic particles and to reduce uncertainty from energy.

II. EXPERIMENT AND SIMULATION

A. LHAASO-KM2A prototype array

A prototype array of about 1% the size of KM2A was constructed at the YBJ cosmic ray observatory, where the altitude is about 4300m. It had been in stable operation from November 2014 to March 2016. This detector array consists of 39 EDs and 2 MDs. 39 EDs are uniformly distributed with the same spacing (15 m) as in KM2A, and 2 MDs are placed into the array. The layout of the arrangement for the array is shown in Fig. 1.

The ED is a kind of scintillator detector with wavelength-shifting fiber to deliver scintillation light to PMT. The area of an ED unit is about 1 m^2, and the time resolution is better than 2 ns. A detailed description of ED is given in [32]. The ED array provides trigger for shower events. When more than 4 EDs are fired instantaneously within a time window of 200 ns, the array is triggered and all hits from both EDs and MDs in a time window of 10 us centered at trigger time are acquired and stored for off-line analysis [33]. ED array is also used to reconstruct the direction and core of shower as well as to measure the number of electromagnetic particles.

The engineering array was proposed to study the performance of detector, and there were many artificial or unexpected factors may lead to abnormal data acquisition in operation, so only data files taken during regular operation period was used in this analysis. The total data used in the analysis accounts for about 324 days. The long

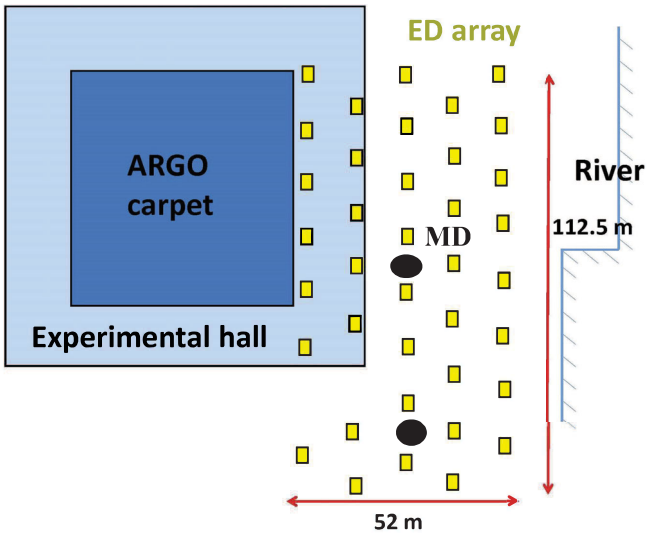

FIG. 1. Layout of arrangement for LHAASO-KM2A prototype array. Black circles and yellow rectangles correspond to MDs and EDs.

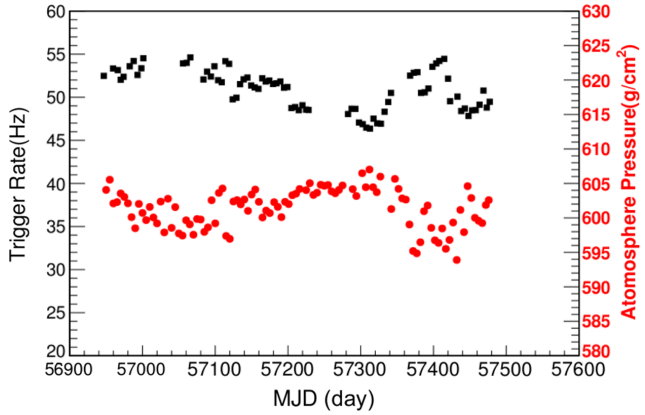

FIG. 2. Long time stability of event trigger rate (black) and atmosphere pressure (red). Each point is an average of data for 5 days.

time stability of event rates for ED array is shown in Fig. 2. The event rates is about 50 Hz, and it follows the change of atmosphere pressure as expected [34].

The MD is a kind of water Cherenkov detector, which has an effective area about 36 m^2. The muon detector is under shielding of 2.5 m thick overburden soil to prevent low energy electromagnetic particles from reaching water, and the threshold for $\mu^{\pm}$ is about 1 GeV. MD has a wide dynamic range up to 10000 particles, which enables to measure the muon content in a large energy range without saturation. The details about MD are described in [33]. Owing to the influence from punch-through effect, which will be discussed in detail in Sec. III, only the muon detector at the center of the array is used in analysis. The performance of MD is monitored by measuring atmosphere background muons. The long time stability of background signal rate for muon detector unit is shown in Fig. 3. The rate changes with different seasons, which is a very slow modulation effect, and the smooth distribution of single rate implies a stable operation condition for muon detector.

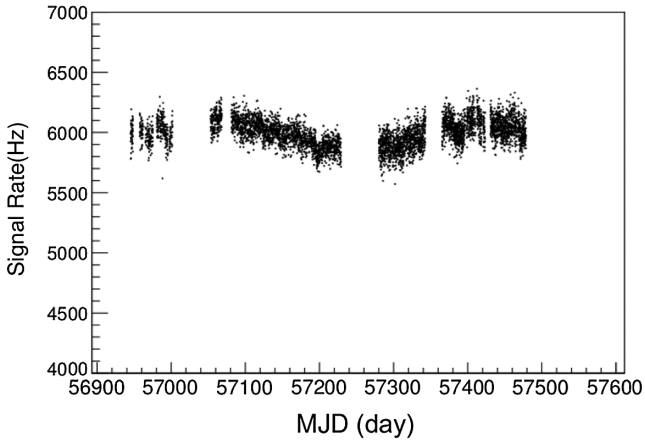

FIG. 3. Long time stability of background signal rate for muon detector. One point corresponds to one data file.

B. Simulation

All processes from shower development in atmosphere to interactions in detectors are simulated. Samples of primary cosmic rays are generated in the energy range from 10 TeV to 100 PeV for proton and iron separately with zenith angles in the interval of 0° to 60°. The composition of cosmic rays in this energy range is not well-known and changes with energy. To simplify the simulation we have modeled the primary cosmic composition using pure proton and iron to represent two extreme mass compositions. A typical power law energy spectrum has been adopted with spectral index 2.7 below 3 PeV and 3.0 above 3 PeV [35]. The core of each shower is randomly assigned with larger radius for higher energy range, which ensures the sampling area is large enough to contain almost all events that can trigger the array. The development of EAS in atmosphere is simulated based on CORSIKA [36] event generator incorporating QGSJETII-04 [37] for the hadronic interaction model. When particles arrive at detectors, the remaining processes are simulated by a GEANT4-based simulation procedure. The details about this GEANT4-based procedure can be found in [38].

III. ANALYSIS METHOD

The number of vertical equivalent muons ($N_{\rm vem}$) for a MD hit is proportional to the signal charge, which can be calculated as:

$$N_{\rm vem} = \frac{Q_{\rm MD}}{Q_V}, \tag{1}$$

where $Q_{\rm MD}$ and Q_V are the charges for the detected hit and single vertical muon separately. Q_V is calibrated by selecting vertical showers. Similarly, the number of particles detected by electromagnetic detector is defined as:

$$N_e = \frac{Q_{\rm ED}}{Q_{\rm MIP}}. \tag{2}$$

Here $Q_{\rm ED}$ is the charge for ED hit, and $Q_{\rm MIP}$ is the charge for minimum ionization particle (MIP), which is also a calibration parameter. The details about detector calibration can be found in [39]. The number of particles detected by the array is a sum of particles detected by each detector:

$$Np_{\rm array} = \sum_{i=1}^{N} N_e^i \tag{3}$$

where N_e^i is the number of particles detected by ith ED.

The muon production in EAS is largely influenced by the primary energy of shower, which consequently leads to an inaccurate prediction of number of muons arriving at muon detectors. This uncertainty is reduced by using $Np_{\rm array}$ to constrain primary energy. It can be referred from Fig. 4 that

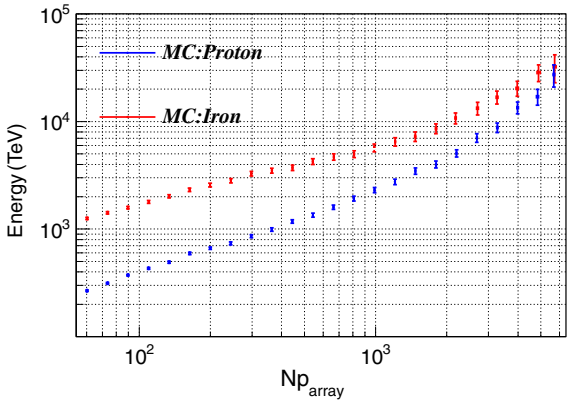

FIG. 4. Primary energy as a function of Np_{array}. The error bar refers to the error of mean value.

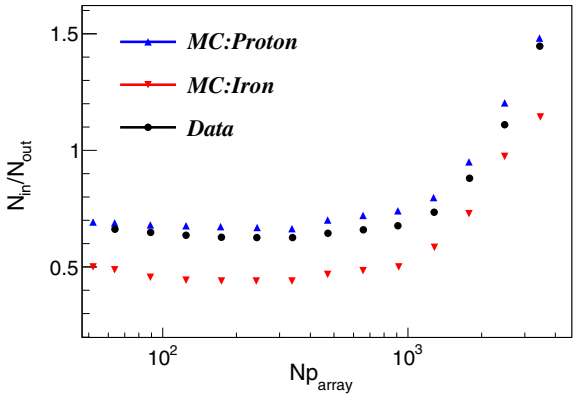

FIG. 5. $N_{\text{in}}/N_{\text{out}}$ as a function of Np_{array} for both simulation and data.

the energy increases with larger Np_{array}, and showers with different energy can be separated statistically. Limited by the dynamic range of electromagnetic detectors, the curves become steeper above thousands of particles.

One challenge for this analysis arises from guarantee of high purity of detected muons, which is polluted by high energy electromagnetic particles and hadrons near shower core that also have chances to arrive at detector despite there is 2.5m burying soil. These high energy particles can also cause a subshower in the soil, which may lead to a much larger signal comparing to muons, and we define this influence as punch-through effect.

Punch-through effect can be reduced by selecting showers with cores away from muon detector due to a steeper lateral distribution for electromagnetic particles comparing to muons. However, limited by the area of the array and the number of detectors, only a small fraction of secondary particles within a shower can be detected by detectors, thus the cores of showers cannot be reconstructed precisely especially for showers with cores out of the array. Considering the position of one muon detector is very close to the center of the array, the distance from shower core to this detector can be ensured by selecting showers with cores out of array, which is called "out" events. In practice, all EDs are divided into two groups. The detectors at the edge of the array are defined as outer detectors while the others are defined as inner detectors. If the number of particles detected by outer detectors is larger than that detected by inner detectors, this shower is labeled as "out" events, otherwise the shower is defined as "in" events. Only showers labeled as "out" events are used in this analysis.

The ratio of "in" array events to "out" array events as a function of Np_{array} is shown in Fig. 5 for both simulation and data to illustrate the similarity of data and Monte Carlo. The events with large number of particles are contributed by high energy events with cores close to the center of the array, and these events are more likely to be "in" evens, thus the ratio will increase correspondingly.

Punch-through effect can also be reduced by selecting more declined showers in which the electromagnetic components are deeper attenuated in atmosphere. The direction of shower can be obtained by fitting the relative arrival time of secondary particles at detectors [39]. The good agreement between simulation and experiment on angle reconstruction can be illustrated in Fig. 6. Only showers with zenith angles in the interval of 40° to 55° are used in this analysis.

Polluted by the punch-through effect, the N_{vem} is larger than the number of simulated muons ($N\mu_{\text{mc}}$). However, the N_{vem} will approach to $N\mu_{\text{mc}}$ if the punch-through effect is diminished, and $N\mu_{\text{mc}}$ can be reconstructed using N_{vem}. The muon reconstruction algorithm is validated in a test with simulation events. The relationships between Np_{array} and $N\mu$ for both simulated muons and reconstructed muons ($N\mu_{\text{rec}}$) are shown in Fig. 7 respectively. It can be seen that there is a good agreement between reconstruction muons and simulated muons at range for Np_{array} above 50 and less than 5000 and proton and iron are well separated, which implies that N_μ/N_e is a very powerful tracer for mass separation. The $N\mu_{\text{rec}}$ is obviously larger than the $N\mu_{\text{mc}}$ at range for Np_{array} above 5000, which is caused by

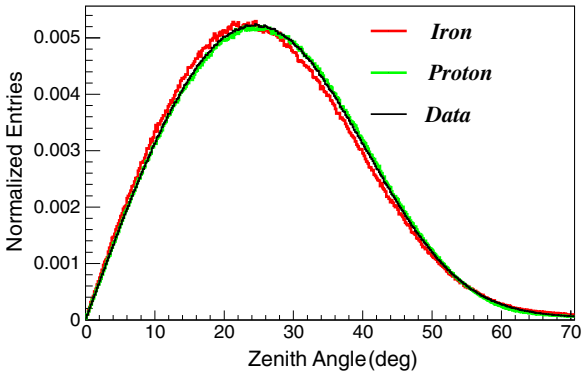

FIG. 6. The normalized zenith angle distribution for simulation and experiment.

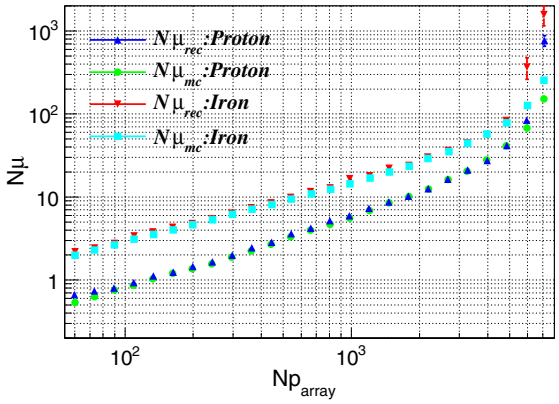

FIG. 7. N_μ as a function of Np_{array}. The point represents the mean value of Np_{array} and N_μ, and the error bar represents the statistical error for mean value.

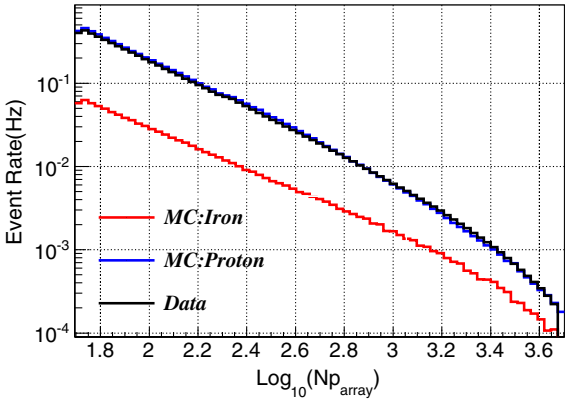

FIG. 9. The measured distribution of Np_{array} (black) compared with the values obtained from simulations with proton (blue) and iron (red) primary cosmic rays. Only events with Np_{array} below 5000 is plotted, which are used in this analysis.

punch-through effect. Thus only events with Np_{array} less than 5000 and above 50 are considered. There were about one billion five hundred million events that triggered the array and only 6.8 million events passed final selection criteria.

IV. RESULTS

Distributions related to this analysis are derived in the same way both for data and simulation to obtain a direct comparison. The model prediction of distribution of N_{vem}, which is scaled by the total exposure time, is shown in Fig. 8 together with experimental data. The showers are selected with Np_{array} above 50. It can be seen that if there is no cut applied to reduce punch-though effect, the N_{vem} is much larger than $N\mu_{\text{mc}}$ (as shown in Fig. 7). The total exposure time for simulation is estimated by summing the individual fluxes of main chemical elements at 1 TeV where measurements are most precise. The flux is estimated to be about $0.225(\text{m}^2\,\text{s}\,\text{sr}\,\text{TeV})^{-1}$ [35].

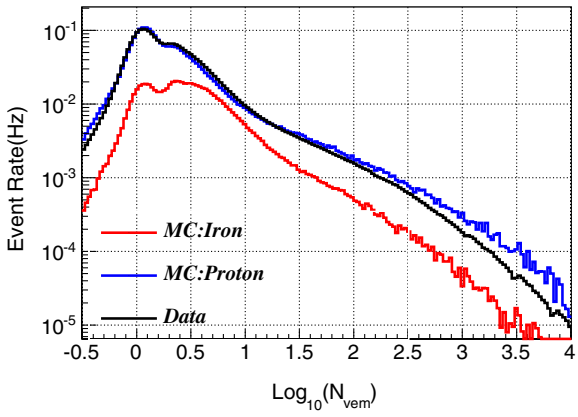

FIG. 8. The measured distribution of N_{vem} (black) compared with the values obtained from simulations with proton (blue) and iron (red) primary cosmic rays.

The shower size for heavy primaries is smaller compared to light primaries at same energy which leads to a higher trigger threshold for iron than proton, it can be seen in Fig. 8 that the flux for iron is much smaller and the experimental data can be well described by simulation, indicating that the simulation procedure is successful in describing all the interaction processes for different particles (including punch-through effect). The distribution of number of particles detected by array is shown in Fig. 9. The distribution is scaled in the same way as for muons, and the simulation results also agree well with data.

Based on the above works, we tried to describe the relationship between N_μ and Np_{array} in large energy range. The results for both experiment and simulation is shown in Fig. 10. At lower energies, the experimental data is parallel with the proton line, which means there is no clear change of composition and the data can be well described by simulation. However, with the increase of Np_{array}, the gradient $dN_\mu/dNp_{\text{array}}$ is larger for data compared to

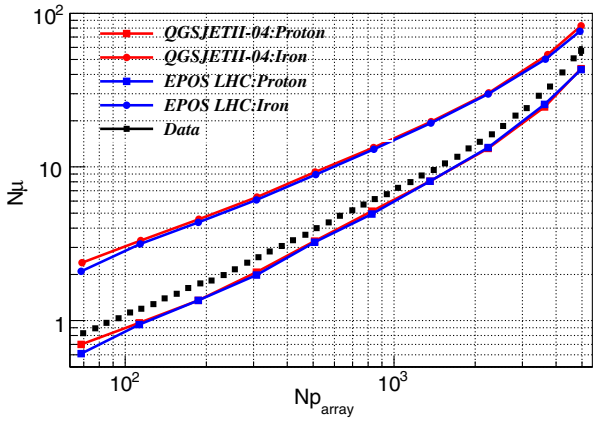

FIG. 10. Number of muons (N_μ) as a function of number of electromagnetic particles (Np_{array}). Data is shown in black point. Simulation results are shown for EPOS-LHC and QGSJETII-04 models separately (blue and red).

proton showers, which may suggest a transition from light to heavy elements. It happens exactly at the energy range around the "knee" region (about several PeV for proton) where primary composition starts to change [40,41]. In addition, there is no obvious excess of muon abundance at least up to 10 PeV considering the primary mass uncertainty. We also repeated the simulation using EPOS LHC hadronic interaction model, and it is found that the two models agree well in this energy interval.

It should be noted that due to the limited number of detectors this result is only a rough conclusion about hadronic interaction model, and more precise measurements should be performed by upcoming full array, which can also extend the energy range to 100 PeV. Furthermore, with the collaboration of different kinds of detectors in LHAASO we can perform a combined analysis using more secondary products, which are expected to give stricter constraints on hadronic interaction models.

V. DISCUSSION AND CONCLUSION

We present a combined measurement of muons and electromagnetic particles from LHAASO-KM2A prototype array. The selected data is equivalent to about one year live time. The latest hadronic interaction model is used to describe the development of shower in atmosphere and the interactions in detector are simulated by a GEANT4-based procedure.

The good agreement between simulation and experiment on several distributions demonstrates the success of this new-developed GEANT4-based simulation procedure in describing the interactions in detector and the reliability of data. Based on these works, we try to describe N_μ/Np_{array} at large energy range using this simulation framework. As a result, the data agrees with the simulation at low energies. While with the increase of energy, there is a clear transition from light mass to heavier mass around "knee" region, and the data can be described by simulation at least up to 10 PeV. EPOS LHC model is also used to repeat the simulation, and the results from the two models agree well, which may be benefited from the high altitude of the experiment and the progress in models. The results can also give insights on the ability of N_μ/N_e for mass separation and hadronic interaction model test. However, limited by the number of detectors we can only draw a rough conclusion about composition and hadronic interaction models, and more precise measurements should be performed by future full array. With the intense construction of LHAASO, the full array together with other detectors will be in operation in the upcoming years, which will give stricter constraints on hadronic interaction models.

ACKNOWLEDGMENTS

This work is partly supported by NSFC (No. 11575203, No. 11635011, No. 11605208 and No. 11405181) and the Knowledge Innovation Fund of the Institute of High Energy Physics of the Chinese Academy of Sciences (IHEP), Beijing.

[1] G. B. Gelmini, J. Phys. Conf. Ser. **171**, 012012 (2009).
[2] W. D. Apel *et al.*, Adv. Space Res. **53**, 1456 (2014).
[3] J. C. Arteaga-Velázquez *et al.*, Eur. Phys. J. Web Conf. **52**, 07002 (2013).
[4] R. Engel, Nucl. Phys. B, Proc. Suppl. **151**, 437 (2006).
[5] J. Knapp, D. Heck, S. J. Sciutto, M. T. Dova, and M. Risse, Astropart. Phys. **19**, 77 (2003).
[6] G. Wilk and Z. Włodarczyk, J. Phys. G Nucl. Phys. **38**, 085201 (2011).
[7] A. Petrukhin, Nucl. Instrum. Methods Phys. Res., Sect. A **742**, 228 (2014).
[8] G. Rodriguez, Eur. Phys. J. Web Conf. **53**, 07003 (2013).
[9] T. Abu-Zayyad *et al.*, Phys. Rev. Lett. **84**, 4276 (2000).
[10] A. V. Glushkov, I. T. Makarov, M. I. Pravdin, I. E. Sleptsov, D. S. Gorbunov, G. I. Rubtsov, and S. V. Troitsky, JETP Lett. **87**, 190 (2008).
[11] R. Jörg and R. Hörandel, Nucl. Phys. B, Proc. Suppl. **122**, 455 (2003).
[12] T. Antoni *et al.*, Astropart. Phys. **24**, 1 (2005).
[13] T. K. Gaisser, Nucl. Part. Phys. Proc. **279–281**, 47 (2016).
[14] Y. Fomin, N. Kalmykov, I. Karpikov, G. Kulikov, M. Kuznetsov, G. Rubtsov, V. Sulakov, and S. Troitsky, Astropart. Phys. **92**, 1 (2017).
[15] J. Ridky and P. Travnicek, Nucl. Phys. B, Proc. Suppl. **138**, 295 (2005).
[16] V. Avati, L. Dick, K. Eggert, J. Ström, H. Wachsmuth, S. Schmeling, T. Ziegler, A. Brühl, and C. Grupen, Astropart. Phys. **19**, 513 (2003).
[17] M. Rybczyński, Z. Włodarczyk, and G. Wilk, Nucl. Phys. B, Proc. Suppl. **151**, 341 (2006).
[18] J. Ridky, Nucl. Phys. B, Proc. Suppl. **110**, 481 (2002).
[19] L. A. Anchordoqui, H. Goldberg, and T. J. Weiler, Phys. Rev. D **95**, 063005 (2017).
[20] J. Ebr, P. Nečesal, and J. Ridky, Astropart. Phys. **90**, 37 (2017).
[21] S. Ostapchenko, Eur. Phys. J. Web Conf. **52**, 02001 (2013).
[22] S. Mollerach and E. Roulet, Prog. Part. Nucl. Phys. **98**, 85 (2018).
[23] T. A. collaboration, J. Cosmol. Astropart. Phys. 01 (2016) 032.

[24] A. Aab *et al.* (Pierre Auger Collaboration), Phys. Rev. Lett. **117**, 192001 (2016).
[25] A. Aab *et al.* (Pierre Auger Collaboration), Phys. Rev. D **91**, 032003 (2015).
[26] R. U. Abbasi, M. Abe, T. Abuzayyad, M. Allen, R. Azuma, E. Barcikowski, J. W. Belz, D. R. Bergman, and S. A. Blake, Phys. Rev. D **98**, 022002 (2018).
[27] W. Apel *et al.*, Astropart. Phys. **95**, 25 (2017).
[28] G. Di Sciascio (LHAASO Collaboration), Nucl. Part. Phys. Proc. **279**, 166 (2016).
[29] S. Cui, Y. Liu, Y. Liu, and X. Ma, Astropart. Phys. **54**, 86 (2014).
[30] H. He, Radiation Detection Technology and Methods **2**, 7 (2018).
[31] H. Lv, X. Sheng, H. He, J. Liu, Z. Zhang, C. Hou, and J. Zhao, Nucl. Instrum. Methods Phys. Res., Sect. A **781**, 34 (2015).
[32] J. Zhao, J. Liu, X.-D. Sheng, H.-H. He, Y.-Q. Guo, C. Hou, and H.-K. Lü, Chin. Phys. C **38**, 036002 (2014).
[33] X. Zuo, G. Xiao, S. Feng, X. Li, C. Li, B. Hong, J. Chang, W. Wang, M. Gu, F. Li, J. Liu, H. Lv, X. Sheng, S. Zhang, H. Li, G. Gong, and H. He, Nucl. Instrum. Methods Phys. Res., Sect. A **789**, 143 (2015).
[34] J. Liu, X.-D. Sheng, H.-H. He, J. Zhao, J.-F. Chang, M.-H. Gu, C. Hou, and H.-K. Lü, Chin. Phys. C **38**, 026001 (2014).
[35] J. R. Hörandel, Astropart. Phys. **19**, 193 (2003).
[36] D. Heck, J. Knapp, J. N. Capdevielle, G. Schatz, and T. Thouw, *CORSIKA: A Monte Carlo Code to Simulate Extensive Air Showers* (Forschungszentrum Karlsruhe GmbH, Karlsruhe, Germany, 1998).
[37] S. Ostapchenko, Nucl. Phys. B, Proc. Suppl. **151**, 143 (2006).
[38] S. Chen *et al.*, Nuclear Electronics and Detection Technology **37**, 11 (2017).
[39] H. Lv, H. He, X. Sheng, J. Liu, S. Chen, Y. Liu, C. Hou, J. Zhao, Z. Zhang, S. Wu, and Y. Wang, Astropart. Phys. **100**, 22 (2018).
[40] W. D. Apel, J. C. Arteagavelazquez, K. Bekk, M. Bertaina, J. Blumer, H. Bozdog, I. M. Brancus, P. Buchholz, E. Cantoni, and A. Chiavassa, Phys. Rev. Lett. **107**, 171104 (2011).
[41] S. F. Berezhnev, N. M. Budnev, O. A. Gress, A. N. Dyachok, S. N. Epimakhov, A. V. Zagorodnikov, N. N. Kalmykov, N. I. Karpov, V. A. Kozhin, and E. N. Konstantinov, Bull. Russ. Acad. Sci. Phys. **79**, 344 (2015).